Desalination and Water Treatment
www.deswater.com

doi:10.5004/dwt.2017.20873

83 (2017) 294–305
July

Calcium alginate-organobentonite-activated carbon composite beads as a highly effective adsorbent for bisphenol A and 2,4,5-trichlorophenol: kinetics and equilibrium studies

Nassima Djebri[a,b,*], Nadia Boukhalfa[b], Mokhtar Boutahala[b,*], Didier Hauchard[c], Nacer-Eddine Chelali[a], Abdelkrim Kahoul[d]

[a]*Laboratoire Matériaux et systèmes Electroniques (LMSE), Faculté des Sciences et de la Technologie, Université de Bordj Bou Arreridj, El Annasser, 34000 BBA, Algérie, email: nessmadjebri@yahoo.fr (N. Djebri)*
[b]*Laboratoire de Génie des Procédés Chimiques (LGPC), Faculté de Technologie, Université Ferhat Abbas Sétif-1, 19000 Sétif, Algérie, email: mboutahala@yahoo.fr (M. Boutahala)*
[c]*Ecole Nationale Supérieure de Chimie de Rennes, CNRS UMR 6226, 13 allée de Beaulieu, CS 50837, 35708 Rennes Cedex 7, France*
[d]*Laboratoire d'Energétique et d'Electrochimie du Solide (LEES), Département de Génie des Procédés, Faculté de Technologie, Université Ferhat Abbas, Sétif-1- 19000, Algérie*

Received 18 April 2017; Accepted 27 April 2017

ABSTRACT

Today toxic phenolic compounds are a major source of pollution and are mainly the result of various industrial wastes such as plastics, polymers, insecticides, etc. In this context, the originality of our study is a first as we used a new composite material assembled by mixing activated carbon (*AC*), organo activated bentonite (*OAB*), and alginate (*A*).The prepared adsorbent materials were characterized by scanning electron microscopy (SEM), Fourier transform infrared spectroscopy (FTIR), and point of zero charge (pH_{PZC}). The influence of various factors such as contact time, pH, adsorbate concentration, and temperature on the adsorption of bisphenol A (BPA) and 2,4,5-trichlorophenol (TCP) has been investigated. The equilibrium data were fitted well by Freundlich isothermal model and the maximum adsorptions of BPA and TCP onto alginate/organo activated bentonite/activated carbon beads (*A-OAB-AC*), were 368.2 and 385.1 $mg{\cdot}g^{-1}$, respectively. The adsorption of BPA and TCP was observed to follow pseudo-second order mechanism as well as the thermodynamic parameters confirm also endothermic spontaneous and physiosorption processes. In addition, the resulting adsorbent reusability was demonstrated by at least six cycles, indicating that the *A-OAB-AC* can be used as a promising adsorbent for removal of toxic pollutants from aqueous solutions.

Keywords: Removal; Alginate; Organobentonite; Activated carbon; Composite; Toxic pollutants

1. Introduction

Increased industrial activities have resulted in the generation of various types of toxic compounds which are the main cause of water pollution on a global scale. The type of pollutants present in wastewater mainly depends on the nature of the industry [1,2]. However, some of the common pollutants generally present in effluents are heavy metals, dyes, phenols, insecticides, pesticides, detergents and a wide spectrum of aromatics. These pollutants can be toxic to aquatic life and can cause natural waters to be unfit as potable water sources [3–5]. Among these toxic phenolic compounds, bisphenols (such as bisphenol-A) and chlorophenols (such as 2,4,5-trichlorophenol) which are widely used in industrial and agricultural activities [3,4]. Their adverse effects on the reproductive functions of aquatic species and influence on humans have been observed worldwide. Indeed, it is necessary to remove these pollutants from wastewaters before dis-

*Corresponding author.

Presented at the First International Symposium on Materials, Electrochemistry and Environment (CIMEE 2016), 22–24 September 2016, Tripoli, Lebanon

charge into the environment [6]. In order to keep waters free from toxic pollutants, different purification methods such as microbial degradation, adsorption, chemical oxidation, solvent extraction, reverse osmosis, and irradiation [6–11] are used for removing these compounds with varying degree of success, to the treatment of water and wastewater. However, these technologies have shown some significant disadvantages which include high capital costs, high reagents and/or energy requirements, insufficient removal of pollutants, and generation of toxic sludge or other waste products that require further safe disposal [5,12].

Among these ways, adsorption has been proved more effective and attractive for the treatment of industrial wastes [10,13]. Adsorption is also a cheap and highly effective method in the removal of pollutants from wastewaters. Activated carbon (AC) has been proved to be an effective adsorbent for the removal of a wide variety of toxic pollutants from aqueous or gaseous media [14,15]. It is widely used due to its exceptionally high surface area, well-developed internal microporosity, and wide spectrum of surface functional groups [12].

The wastewater materials and agriculture wastes are assumed to be low-cost adsorbents due to their most abundance in nature and with many surface functional groups. The raw agricultural wastes such as coconut husks [16], fruit peels [15], coffee grounds [17] olive mill [18,19] etc. have been used as adsorbents for purifications and removal of toxic pollutants.

Clays are widely used to study the adsorption of pollutants from water. These clays are chosen to avoid pollutant release into the environment owing to their high surface areas, low cost and ubiquitous presence in most soils [20,21]. Bentonite as a representative clay mineral is mainly composed of montmorillonite, a 2:1 type of aluminosilicate. Bentonites are highly valued for their adsorptive properties. Affinity of some pollutants to bentonite is also of special interest of adsorption applications [21].

Sodium alginate is a polysaccharide extracted from seaweed, performed excellently in the removal of pollutants from water. Alginate has some unique properties such as hydrophilicity, biocompatibility, and non-toxicity [5,22]. The important feature of alginate is to have high affinity toward several compounds to its abundance of carboxylic acid groups, instead of having other functional groups such as sulfonic acid and hydroxyl groups [23,24].

To prepare the composites adsorbents, both inorganic and organic compounds may be used as binding materials. Mixture materials may offer combined properties as to provide an improvement upon thermal, mechanical and porosity properties compared with the homogenous characteristics of the bare individual activated carbon, bentonite and alginate polymer components [21,24].

The main objective of the present work is to study and evaluate a new composite material (*A-OAB-AC*) for the removal of bisphenol A and 2.4.5-trichlorophenol from an aqueous solution. Further, the effect of pH, contact time, initial concentrations of adsorbate and temperature on the extent of adsorption is investigated. Kinetics adsorption data are fitted to pseudo first order, pseudo second order and intraparticle diffusion. Equilibrium adsorption data are fitted to Langmuir and Freundlich isotherms. Further, the adsorbent loaded with bisphenol A and 2,4,5-trichlorophenol is regenerated by elution method.

2. Materials and methods

2.1. Materials

The raw bentonite (*RB*) used in this study was obtained from Hammam Boughrara in Maghnia (West Algeria). The chemical composition of the *RB* was reported in our earlier publication [5]. The surfactant used for the preparation of organoclay is CTAB ($C_{19}H_{42}NBr$, > 98%), which is obtained from Sigma-Aldrich. For preparation of activated carbon, apricot stone was obtained locally (region Setif-Algeria). Bisphenol A (BPA), 2,4,5-Trichlorophenol (TCP)(toxic pollutants selected for this study), sodium chloride, sulfuric acid were also purchased from Sigma-Aldrich. Distilled water was used in all experiments.

2.2. Preparation of organo-acid-activated bentonite (OAB)

The organo-acid-activated bentonite (OAB) was prepared according to the method described in our earlier publication [4]. Briefly, in the first step the purified bentonite was subjected to acid treatment with sulfuric acid H_2SO_4 1 M (1:1 w/w) with stirring and reflux heating (90°C) for 5 h. The resulting solid was washed with distilled water until it was free from sulfate ions, dried at 80°C and named AB. For the second step, AB was treated with cetyltrimethylammonium bromide (CTAB) by adding the amount of the cationic surfactant equivalent to 100% of the value CEC of bentonite. The surfactant was dissolved in 1 L hydrochloric acid (HCl 0.01 N, d = 1.18) at 80°C and stirred for 3 h. 10 g of the sample (AB) were added to the surfactant solution. The dispersion was stirred for 3 h at 80°C. The resulting solid, named OAB, was separated, washed several times with distilled water until the supernatant solution was free from bromide ions and dried at 80°C for 48 h.

2.3. Preparation of activated carbon (AC)

The apricot stone (AS) collected apricot was obtained from Algerian local markets as a precursor. The activated carbon was prepared by chemical activation using phosphoric acid as activating agent according to the previous work [25]. Briefly, the first step, chemical impregnation was carried out in a round-bottom flask reactor, where 20 g of the precursor reacted with a 40wt.% H_3PO_4 solution at a ratio of 1:2 (g AS/g H_3PO_4), stirred for 6 h. After impregnation, the solid was filtered under vacuum to remove the excess of phosphoric acid and calcined at 450°C for 1 h, defining a heating ramp of 10°C/min. The resulting carbon was thoroughly washed with distilled water in order to remove the remaining phosphoric acid until reaching a pH 6.5. Finally, the solid was dried in an oven at 110°C for 24 h. The resulting material was named as *AC* activated carbon.

2.4. Preparation of calcium alginate beads (A)

Solutions of 1% sodium alginate and 4% calcium chloride were prepared separately in deionized water [5]. For preparation of alginate (*A*) beads, a 1% sodium alginate solution was added drop wise by a push-pull syringe pump to a calcium chloride solution. The water-soluble sodium alginate was converted to water-insoluble cal-

cium alginate beads. All beads were then washed with deionized water several times to remove the excess of unbounded calcium chloride from the bead surfaces. The washed beads were then dried and stored in a clean dry glass bottle.

2.5. Preparation of the mixed material (A-OAB-AC)

A solution of 1% sodium alginate was prepared in deionized water in a 250 mL flask with stirring for 2 h. Then 2 g of organo-acid-activated bentonite (*OAB*) and 2 g activated carbon (*AC*) were added, and the mixture was stirred for 24 h at room temperature. The homogenous mixture was dropped by a push-pull syringe pump into a flask containing a $CaCl_2$ (4%, w/v) solution to produce calcium alginate/organo-acid activated bentonite/activated carbon (*A-OAB-AC*) beads. The collected mixture material beads were washed thoroughly, dried and stored in a clean dry glass bottle for subsequent use.

2.6. Characterization of the samples (A, AC, OAB and A-OAB-AC)

The morphological structure of the investigated samples was examined by SEM using a SEM model (JSM-6830LV, JEOL).

FTIR analysis of the samples *A, AC, OAB* was carried out in KBr pellets in the range of 4000–400 cm^{-1} with 4 cm^{-1} resolution using a Mattson 5000 FTIR spectrometer. In addition, the sample *A-OAB-AC* was also analyzed before and after BPA and TCP adsorption.

The pH_{PZC}(point of zero charge) values of *A, AC, OAB* and *A-OAB-AC* (figure not shown) were obtained using published a method [25]. In brief, the initial pHs (pH_i) of aqueous solutions (50 mL) were adjusted to a pH range of 2–10 using HCl or NaOH. Then, 50 mg of adsorbent was added to each sample. The dispersions were stirred for 48 h at 25°C, and the final pH of the solutions (pH_f) was determined. The point of zero charge was obtained from a plot of (pH_f–pH_i) versus pH_i.

2.7. Batch adsorption studies

The adsorption of adsorbates (BPA and TCP) was conducted in a static batch experiment. An aqueous solution of a certain concentration of adsorbate (20–500 mg·L^{-1}) was shaken in bottles of 200 mL capacity with 1 g·L^{-1} of adsorbent *A-OAB-AC* for 96 h. The supernatant liquid was separated out, where the equilibrium concentration of the BPA and TCP was determined using UV/Vis 1700 spectrophotometer at 276 and 290 nm, respectively.

The effect of initial pH on *A-OAB-AC* was examined from pH 2 to 11, at fixed *A-OAB-AC* dosage of 0.2 g, constant initial concentration of 100 mg·L^{-1}, and temperature of 25°C. The pH was adjusted using 0.1 and 1.0 M HCl or NaOH.

Effect of temperature was examined at 15, 25, 35 and 45°C and constant pH of 7.0 and 4.0 for BPA and TCP, respectively. In these experiments, 0.2 g of adsorbent *A-OAB-AC* with 200 mL of 100 mg·L^{-1} of BPA or TCP was employed. After shaking, the adsorption rate was measured. The adsorbed amount at equilibrium, q_e (mg·g^{-1}) was calculated by:

$$q_e = \frac{(C_0 - C_e)\cdot V}{m} \quad (1)$$

The percentage removal (R%) by the adsorbent was described by the following:

$$R(\%) = \frac{(C_0 - C_e)\cdot 100}{C_0} \quad (2)$$

where C_0 and C_e (mg·L^{-1}) are the liquid-phase concentration of BPA or TCP at initial and equilibrium, respectively, V is the volume of the solution (L) and m is the weight (g) of the adsorbent.

2.8. Kinetic study

Effect of time was carried out by contacting 0.2 g of adsorbent with 200 mL bottles of definite concentration of adsorbate (50, 200 and 300 mg·L^{-1} of BPA or TCP). The concentration of adsorbate after recorded time intervals was determined. The adsorption capacity q_t (mg·g^{-1}) at different contact time t (h) was determined using the following equation:

$$q_t = \frac{(C_0 - C_t)\cdot V}{m} \quad (3)$$

where C_t (mg·L^{-1}) is the concentration of BPA or TCP at time t (h) in the solution

2.9. Desorption and regeneration of A-OAB-AC

Desorption study was conducted using ethanol as a desorption eluent. Adsorption was first conducted using the optimal procedure in section 2.7. Then the *A-OAB-AC* with adsorbed BPA or TCP was separated from the solutions. Subsequently, the supernatant solutions were discarded and the *A-OAB-AC* adsorbent was washed with distilled water. Finally, the BPA or TCP were desorbed from the *A-OAB-AC* with 50 mL of ethanol with stirring during 6 h. After desorption process, the beads, with a size of about 1 mm, were washed with distilled water. To investigate the regeneration of the adsorbent, the *A-OAB-AC* was reused in adsorption experiments and the process was repeated for six times. The percentage of desorption of BPA or TCP was calculated by the following equation:

$$R(\%) = \frac{m_{des}}{m_{ads}} \times 100 \quad (4)$$

where m_{des}(mg) and m_{ads} (mg) are the amounts of desorbed and adsorbed BPA or TCP, respectively.

3. Results and discussion

3.1. Characterization results

SEM images were taken at 4000× (Fig. 1a), 150× (Fig. 1b) and 50× (Fig. 1c,d) magnifications to observe the surface

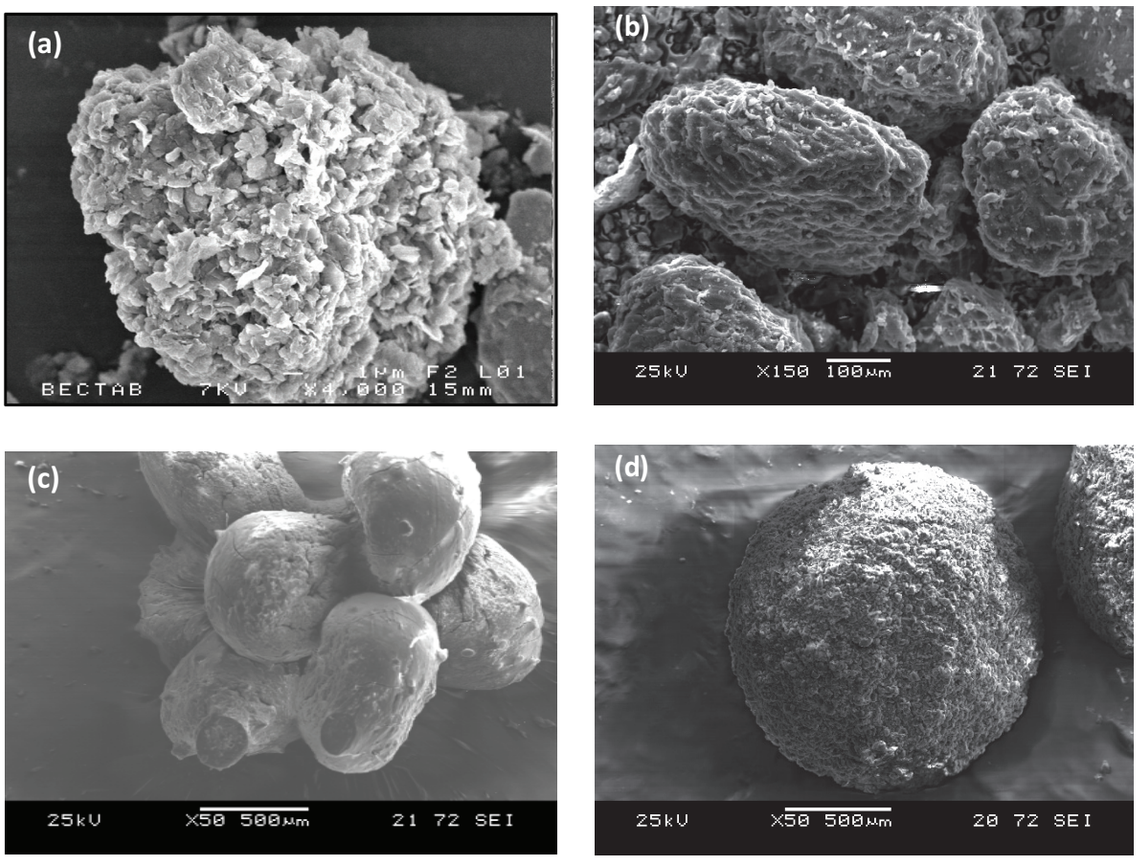

Fig. 1. SEM images of the (a) *OAB*, (b) *A*, (c) *AC* and (d) *A-OAB-AC* samples.

morphologies of *OAB*, *AC*, *A*, and *A-OAB-AC*, as shown in Fig. 1. The surface of *OAB* (Fig. 1a) shows aggregated morphology with a large number of crumpled structure small flakes and the plates become relatively flat layers. More voids are seen due to an increase of basal space in organoclays [4,5], while the surface of activated carbon *AC* (Fig. 1b) is characterized by grooves, irregular ridges and channels which appeared highly undulated due to the presence of intermittently spaced protrusions indicated by bright spots [12,21]. The surface shows an irregular distribution of pore sizes which matched a honeycomb structure of variable hole sizes. This variability in pore size implied a wide surface area for active sites for sorption to potentially take place. The surface of (*A)* beads (Fig. 1c) had a relatively uniform morphology. From Fig. 1d the introduction of *OAB* and AC in the structure of biopolymer, *A*, revealed that the beads have spherical shape, their surface is relatively smooth and has undulations, and shows that the *A-OAB-AC* beads exhibit a bright and clear morphology with a heterogeneous surface.

FTIR spectra of *A, OAB, AC* and *A-OAB-AC* are shown in Fig. 2a. Broad peaks between 3,100 and 3,700 cm^{-1} were due to stretching vibration of O–H bond in hydroxyl groups. FTIR spectrum of alginate (*A*) shows absorption bands at 3,390, 1,618 and 1,412 cm^{-1} that are assigned to vibrations of –OH, and –COO asymmetric stretching, symmetric stretching, respectively. The band at 2,924 cm^{-1} is attributed to the C–H stretching vibration, the band at 1,125 cm^{-1} is due to the C–O stretching of ether groups and the band at 1,065 cm^{-1} is assigned to the C–O stretching of alcoholic groups [5]. In the case of OAB, the bands at 2,925, 2,853, 1,475 and 792 cm^{-1} are assigned to the antisymmetric, symmetric stretching, the scissoring and rocking vibration of methylene group (CH_2) of hexadecyl chain, respectively. These observed FTIR peaks also confirm the intercalation of the surfactant cations into the interlayer galleries of the bentonite. The band at 1,040 cm^{-1} is attributed to the Si–O stretching vibrations of the tetrahedral sheet and the bands at 518 and 465 cm^{-1} are due to Si–O–Al and Si–O–Si bending vibrations. The infrared spectrum of the prepared activated carbon is illustrated in Fig. 2a. The broad absorption band at 3,300–3,600 cm^{-1} with a maximum at about 3,438 cm^{-1} is characteristic of the stretching vibration of hydrogen-bonded hydroxyl groups (from carboxyls, phenols or alcohols) and water adsorbed in the activated carbon. The ν(C–H) stretching bands at 2,922 and 2,850 cm^{-1} (C–H stretching in –CH–) are detectable for the activated carbon. The band at 805 cm^{-1} is due to out of-plane deformation mode of C–H for different substituted benzene rings. The small band at about 1,742 cm^{-1} is usually assigned to C–O stretching vibrations of ketones, aldehydes, lactones or carboxyl groups. The spectrum of the prepared activated carbon also show a band at 1,630 cm^{-1} due to C–C vibrations in aromatic rings. The shoulder at 1,094 cm^{-1} was ascribed

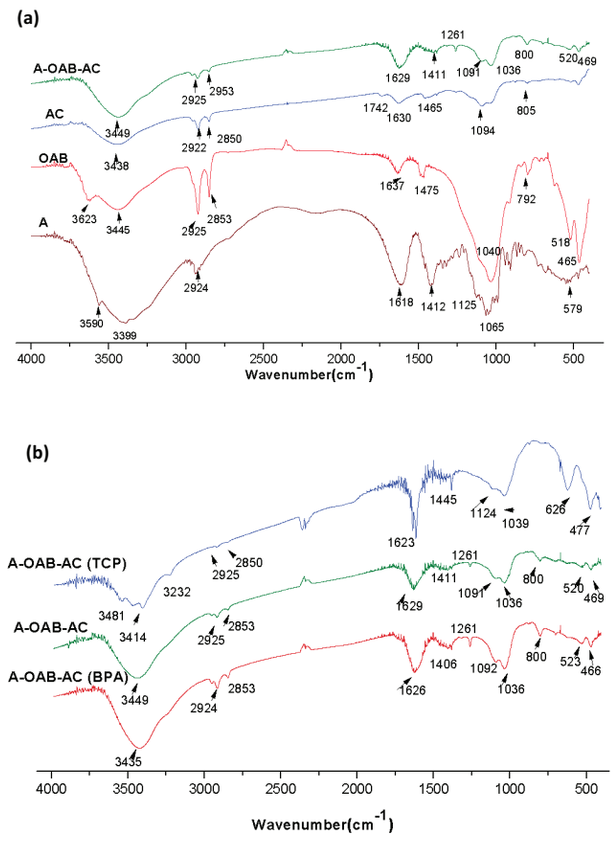

Fig. 2. FTIR spectra of all samples: *A, AC, OAB* and *A-OAB-AC* (a) *A-OAB-AC* before and after adsorption of BPA (*A-OAB-AC* (BPA)) and TCP(*A-OAB-AC*(TCP)) (b).

to ionized linkage P^{+}–O– in acid phosphate esters, and to symmetrical vibration in a P–O–P chain [26]. In the case of*A-OAB-AC*, the wide band at about 3,449 cm^{-1} is due to stretching vibration of O–H (hydroxyl) groups. The bands at 2925, 2,853 and 800 cm^{-1} are assigned to the antisymmetric stretching, symmetric stretching and rocking vibration of methylene group (CH_2) of hexadecyl chain, respectively. Peaks located around 1,629 and 1,036 cm^{-1} could be related to C=C stretching for unsaturated aliphatic structures and –COO alcoholic [27,28] groups, respectively. The vibration band at 1,091 cm^{-1} can be assigned to the stretching C–O vibrations of carboxylate and ether structures, and the bending O–H modes of phenol structures [29]. Also, the bands at 520 and 469 cm^{-1} are characteristic of Al–O stretching and Si–O bending of OAB clay. These results provide clear evidence of the presence of alginate, modified bentonite and also activated carbon in the *A-OAB-AC* adsorbent.

The FTIR spectra of the *A-OAB-AC* loaded with BPA (*A-OAB-AC* (BPA) and TCP (*A-OAB-AC* (TCP)) are given in the same figure (Fig. 2b). These spectra indicate that the peaks due to the *A-AC-OAB* functional groups are slightly affected in their position and intensity. The first change in FTIR spectra as a result of BPA or TCP adsorption is a slight shift of carboxylate anion band from 1,629 cm^{-1} to 1,623 and 1,626 cm^{-1} after adsorption of BPA and TCP, respectively, which could be assigned to the electrostatic binding of phenol to the binding sites. Similarly, the band position of the –OH stretching vibration is shifted from 3,449 to 3,414 (BPA) and 3,435 cm^{-1} (TCP), and the band intensities of OH stretching (3,449 cm^{-1}) vibrations was decreased after TCP adsorption. These phenomena indicate that OH functional groups on the composite materials interacted with hydroxyl groups contained in BPA and TCP resulting in hydrogen bonding [30].

The second change, related to the van der Waals interaction between the phenyl ring of BPA or TCP and –CH_2– group of modified bentonite through hydrogen bonds, can be another mechanism for the adsorption of BPA or TCP onto A-OAB-AC. This may be attributed to the interaction between the functional groups of alginate, modified bentonite and activated carbon with phenolic compounds during the adsorption process. These results confirm the participation of carboxylic, hydroxyl and –CH_2– groups of A-OAB-AC blended beads as potential active binding sites for adsorption of phenolic compounds.

To better understand the adsorption mechanism, the pH_{PZC} points values of *A, AC, OAB* and A-OAB-AC were determined (figure not shown). The point of intersection for which the pH_f–pH_i equals zero was detected as the pH_{PZC} of the adsorbent. The pH_{PZC} of *A*, *AC* and *OAB* were found to be 6.6, 3.0 and 5.9 while $pH_{PZC}$of *A-OAB-AC* was found to be 5.2, which indicates the acid character of the *A-OAB-AC* surface, in agreement with the presence of acid groups from the FTIR results above. Below the pH_{PZC} value, the surface of *A-OAB-AC* is positively charged due to protonation, favoring the adsorption of anions via electrostatic force of attraction. Above the pH_{PZC}, the A-OAB-AC surface has a negative charge which favors the adsorption of cation species.

3.2. Effect of pH

Generally, the pH has an important effect on the adsorption of target compound by affecting the existing form of compound and the charge type and density on the sorbent's surface. In this study, the effect of pH on the adsorption of BPA (pKa = 9.6–10.2) and TCP (pKa = 6.7–6.94) on *A-OAB-AC* material was studied in the pH range of 2.0 to 11.0. The results are shown in Fig. 3. The results showed that the highest removal percentage of BPA and TCP was found at pH 7.0 and 4.0, respectively (80.1% for BPA and 89.6% for TCP). This percentage gradually decreased up to a certain pH (at pH 11.0, 70.6% for BPA and 27.0% for TCP). At a higher pH, the repulsion of the negatively charged BPA or TCP species and the dissociation of functional groups of adsorbent may decrease the interaction of adsorption system. The ionic fraction of the phenols ions increased with increasing pH (pH > pKa), and phenolate became negatively charged as the pH increased, the competitive adsorption of OH^- ions can also result in a decrease in adsorption capacity. In addition, the pH_{PZC} of the *A-OAB-AC* was 5.2. Below pH_{PZC} the *A-OAB-AC* presented a superficial positive charge, and above pH_{PZC} the surface of the *A-OAB-AC* was negatively charged. As can be seen in Fig. 3, adsorption of BPA and TCP occurred when the surface of the *A-OAB-AC* was positively charged. Similar results were also reported by several authors [19,31,32] for the removal of BPA and TCP.

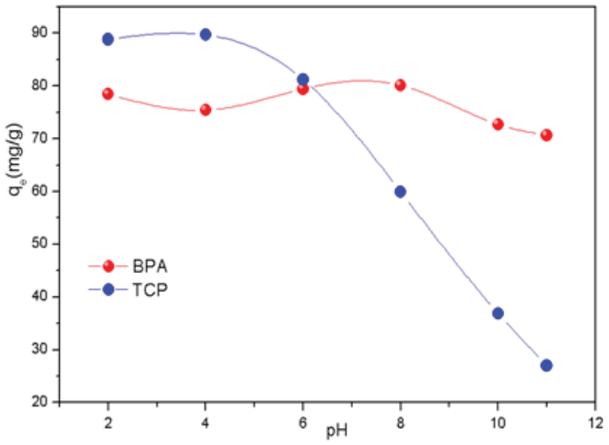

Fig. 3. Effect of solution pH on the adsorption of BPA and TCP on *A-OAB-AC* adsorbent at 25°C.

3.3. Effect of contact time and initial concentration

Fig. 4. shows the effect of contact time at various initial BPA or TCP concentrations on the adsorption capacity of A-OAB-AC. It can be seen that the adsorption capacity increased with increasing contact time and initial concentration of the adsorbate, remaining virtually constant after equilibrium had been attained. This phenomenon was due to the fact that a large number of vacant surface sites was available for adsorption during the initial stage, namely, the external surface sorption or faster sorption stage, and after a lapse of time, the remaining vacant surface sites were difficult to be occupied due to repulsive forces between the solute molecules on the solid and bulk phases, namely, the interior surface sorption or gradual sorption stage. The time necessary to achieve equilibrium increased with increasing adsorbate concentration, being 30, 48 and 51 h for adsorbates (BPA and TCP) concentrations of 50, 200, and 300 mg·L^{-1}, respectively, and the amount of BPA and TCP adsorbed by the A-OAB-AC adsorbent at equilibrium increased from 50.8 to 233.9 mg·g^{-1} and from 37.5 to 296.0 mg·g^{-1} as the initial concentration increased from 50 to 300 mg·L^{-1}. The effect can be attributed to the greater rate of collision rate between BPA or TCP and A-OAB-AC surface at higher initial concentration. This indicates that the initial concentration plays a significant role in the adsorption capacity of BPA and TCP onto A-OAB-AC adsorbent. Similar observations were reported for the adsorption of BPA and TCP [31–34].

3.4. Adsorption kinetic

The kinetic data in this study were applied on pseudo first-order and pseudo second-order models [24]. The pseudo-first order kinetic model is an equation for the adsorption in a solid/liquid system based on the difference between equilibrium adsorption capacity, q_e, and actual solid phase concentration, q_t, measured at a given time t. The linear form of the pseudo-first-order equation is given by Eq. (5) [35]:

$$Ln(q_e - q_t) = \ln q_e - k_1 / t \quad (5)$$

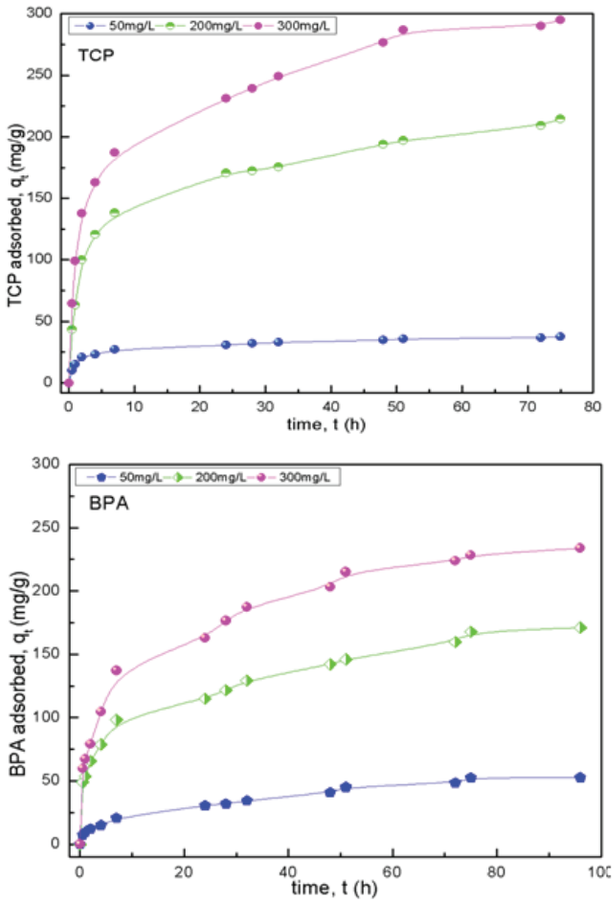

Fig. 4. Effect of contact time and initial concentration on the adsorption of BPA and TCP on *A-OAB-AC* adsorbent at 25°C.

where k_1 (h^{-1}) is the equilibrium rate constant of pseudo-first-order equation. The rate constants are obtained from the straight line plots of $Ln(q_e–q_t)$ vs. t (figure not shown) where the values are given in Table 1.

The pseudo-second-order model is based on the assumption of chemisorption of the adsorbate on the adsorbent [36]. This model is given by Eq. (6):

$$t / q_t = (1 / k_2 q_e^2) + (t / q_e) \quad (6)$$

where k_2 (g·mg^{-1}·h^{-1}) is the rate constant of pseudo-second-order kinetics. The linear plots of t/q_t vs. t (Fig. 5.) were used to obtain the rate parameters given in Table 1.

The results of kinetic adsorption of BPA and TCP by *A-OAB-AC* under various concentrations were calculated from the related plots and the results are listed in Table 1. For both investigated adsorbates, the correlation coefficients for the pseudo-second-order kinetic model were higher than those for the pseudo-first-order model. In addition to the high R^2 values (>0.96 for all tested concentrations), the q_e values estimated from the pseudo-second-order kinetic model were also in agreement with the

experimental values, q_{exp}, for all tested concentrations (Table 1). The two kinetic models describe the uptake behavior of BPA and TCP over the whole adsorption process, however, these models do not account for the diffusion mechanism. Moreover, the overall rate of the BPA and TCP adsorption is likely monitored by chemically sharing of electrons or by covalently exchanging of electrons between adsorbent and adsorbate [37]. Several authors showed the successful application of pseudo-second order model for the representation of experimental kinetics data of pollutants adsorption on various adsorbents [32,35–39].

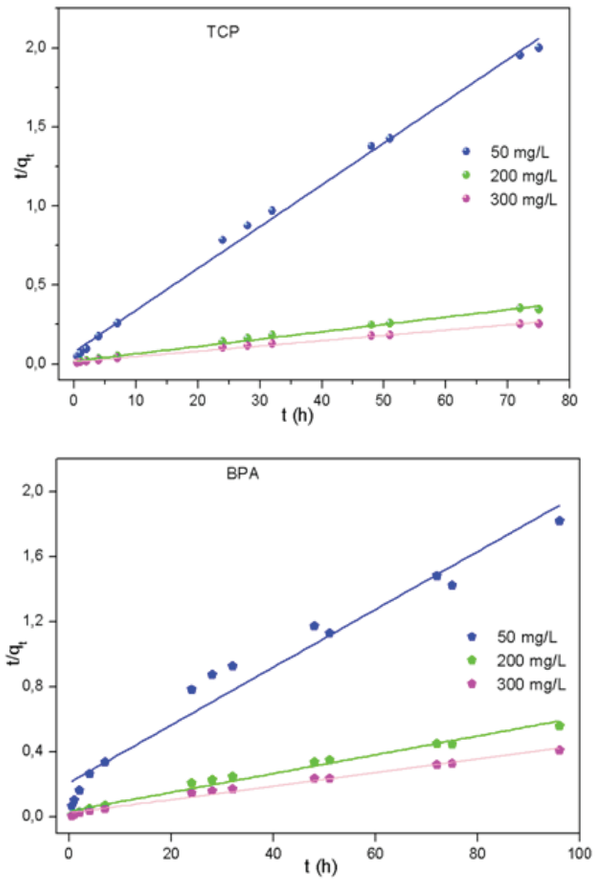

Fig. 5. Pseudo-second-order kinetics for adsorption of BPA and TCP on *A-OAB-AC* at 25°C.

3.5. Adsorption mechanism

Intraparticle diffusion is a transport process involving movement of species from the solution bulk to the solid phase. In a well stirred batch adsorption system, the intraparticle diffusion model is used to describe the adsorption process occurring on a porous adsorbent. The transport of adsorbate from solution to the surface of adsorbent is considered to be completed in following steps: (a) movement of adsorbate from solution to the surface of adsorbate known as film or external diffusion, (b) transfer of adsorbate from boundary layer to surface, (c) diffusion of BPA or TCP molecule to the adsorption sites either by pores diffusion process or through solid surface diffusion mechanism, and (d) adsorption of adsorbate at adsorbent sites.

A plot of the amount of adsorbate adsorbed, q_t (mg·g^{-1}) and the square root of the time, gives the rate constant by calculating the plot slope. This model can be described by the following equation [5]:

$$q_t = k_3\sqrt{t} + C \tag{7}$$

where k_3 (mg·g^{-1}·h$^{-0.5}$) and C are diffusion coefficient and intraparticle diffusion constant, respectively. C is directly proportional to the thickness of the boundary layer [15,37].

Fig. 6 shows a plot of the amount of BPA or TCP adsorbed versus $\sqrt{t}$ or $t^{0.5}$ for different initial concentrations. The regression was not linear over the whole time range, which suggests that more than one mode of adsorption along with intraparticle diffusion, is involved in the BPA and TCP adsorption. The values of K_3 as well as the correlation coefficients, R^2 obtained from the plots are given in Table 2. The values of K_3 generally increased as the initial BPA or TCP concentration increased, which can be attributed to the greater driving force.

As shown in Fig. 6, the plots in this experiment for both adsorbates, for all initial concentrations the data exhibit multi-linear plots (two steps occurred in the process). This suggests that both surface adsorption and intra-particle diffusion were simultaneously occurring during the process and contribute to the adsorption mechanism. The first, sharper portion was the external surface adsorption or the instantaneous adsorption. The second portion was the gradual adsorption stage where intraparticle diffusion was rate-limiting. The R^2 values (Table 2) for the intraparticle diffusion model provide a better fit but not than the pseudo second order kinetic model. Similar observations have been reported in previous studies [20,28,40–43].

Table 1
Pseudo-first and second- order models parameters for BPA and TCP adsorption by A-OAB-AC at 25°C

			Pseudo-first-order model			Pseudo-second-order model		
	C_0	$q_{e,exp}$	$q_{e,cal}$	$k_1{\cdot}10^2$	R^2	$q_{e,cal}$	$k_2{\cdot}10^2$	R^2
BPA	50	50.8	69.7	6.2	0.800	54.3	0.2	0.969
	200	171.8	146.6	4.5	0.904	173.3	0.1	0.983
	300	233.9	176.6	4.2	0.972	240.4	0.1	0.991
TCP	50	37.5	27.8	6.7	0.811	37.8	1.0	0.996
	200	216.4	210.7	1.4	0.830	215.1	0.1	0.993
	300	296.0	191.9	4.2	0.951	296.6	0.1	0.994

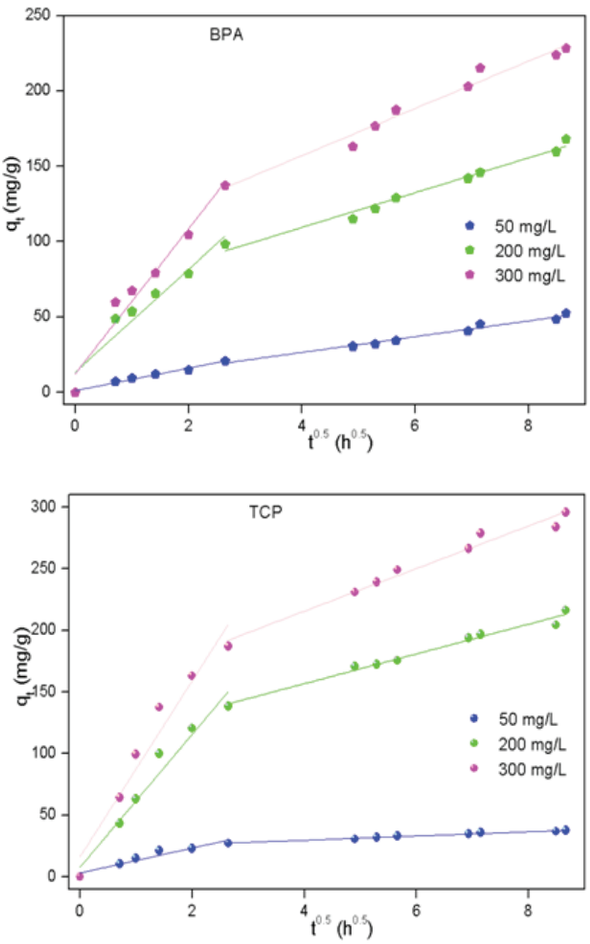

Fig. 6. Intra-particle diffusion plots for the adsorption of BPA and TCP by *A-OAB-AC* adsorbent at 25°C.

Table 2
Intraparticle diffusion parameters for adsorption of BPA and TCP by A-OAB-AC at 25°C

Toxic pollutants	C_0	Intra-particle diffusion model			
		Step 1		Step 2	
		K_3	R^2	K_3	R^2
BPA	50	1.2	0.979	3.0	0.969
	200	13.4	0.910	7.7	0.985
	300	13.5	0.953	16.1	0.942
TCP	50	5.6	0.913	1.8	0.956
	200	12.9	0.953	11.4	0.956
	300	16.1	0.939	15.9	0.948

3.6. Adsorption isotherm

To optimize the design of an adsorption system for the adsorption of adsorbates, it is important to establish the most appropriate correlation for the equilibrium curves. The adsorption isotherm results for BPA and TCP onto *A-OAB-AC* were fitted using two famous isotherm models (Langmuir and Freundlich models) to evaluate a suitable model for describing the adsorption process.

The Langmuir equation hypothesizes that the adsorption process happens on a homogeneous surface in the monolayer pattern, and the sorption energies are equivalent. The Langmuir equation can be expressed as follows [44]:

$$q_e = (q_m K_L C_e) / (1 + K_L C_e) \quad (8)$$

Eq. (8) can be rearranged by a linear equation as:

$$C_e / q_e = C_e / q_m + 1 / K_L q_m \quad (9)$$

where C_e (mg·L^{-1}) is the equilibrium concentration of BPA and TCP, q_m (mg·g^{-1}) represents the maximum adsorption capacity, K_L (L·mg^{-1}) is the Langmuir constant related to the energy of adsorption and represents the affinity within adsorbent and adsorbate.

The Freundlich equation hypothesizes that the adsorption process happens on a heterogeneous surface in the multilayer pattern of varied affinities. It is based on the fact that, the stronger binding sites are occupied first and that the binding strength decreases as the degree of site occupation increases, and it is expressed as [45]:

$$q_e = K_F C_e^{1/n} \quad (10)$$

Eq. (10) can be rearranged by a linear form as:

$$\log(q_e) = \log(k_F) + \frac{1}{n}\log(C_e) \quad (11)$$

where n is the Freundlich constant reflecting the intensity of the adsorption, K_F ((mg·g^{-1}) (L·mg^{-1})$^{1/n}$) is a constant indicating the adsorption capacity of the adsorbent. The calculated constants of the two isotherm equations along with R^2 values for both components are presented in Table 3.

The highest values of the R^2 for both Langmuir and Freundlich models showed that the adsorption isotherms of BPA and TCP by *A-OAB-AC* (Table 3, Fig. 7.) were represented by the two models, but Freundlich model was better, which also supports the proposed physisorption mechanism, and two kinds of organic molecules are bonded as multilayer on the surface of the *A-OAB-AC*. The monolayer saturation capacities were obtained at 25°C to be 368.2 and 385.1 mg·g^{-1} for BPA and TCP onto *A-OAB-AC* respectively. From Table 3, it is shown that the K_F value of TCP adsorption is larger than this of BPA adsorption, which implies that the adsorption of TCP by this adsorbent is much stronger than the adsorption of BPA. It was also observed that the values of $1/n$ were all less than 1.0, indicating that the BPA and TCP adsorption onto the *A-OAB-AC* was favorable [34]. Similar results were obtained using composite materials [29,46,47].

3.7. Effect of temperature

The effect of temperature on the adsorption capacity of BPA and TCP onto *A-OAB-AC* was studied at pH≈6.5 employing adsorbent dose of 1 g·L^{-1} under different tem-

Table 3
Fitting parameters of adsorption model isotherm for BPA and TCP onto A-OAB-AC

Isotherm model	BPA	TCP
Langmuir		
q_{max} (mg·g^{-1})	368.2	385.1
$K_L \cdot 10^2$ (L·mg^{-1})	1.55	2.77
R^2	0.978	0.986
Freundlich		
K_F ((mg·g^{-1}) (L·mg^{-1})$^{1/n}$	16.81	26.23
$1/n$	0.57	0.53
R^2	0.999	0.992

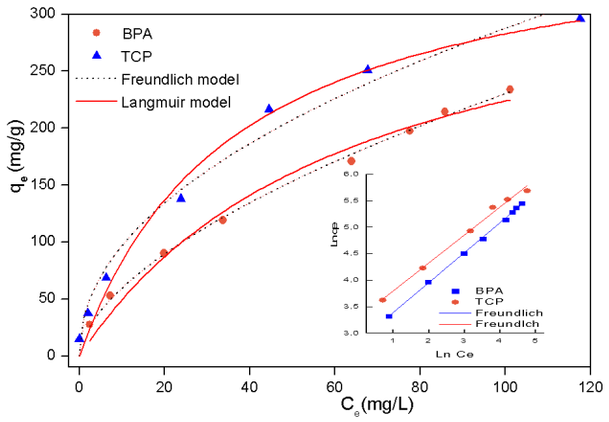

Fig. 7. Langmuir and Freundlich isotherms for BPA and TCP adsorption on *A-OAB-AC* at 25°C.

peratures at 15, 25, 35 and 45°C (figure not shown). The adsorption capacity of the *A-OAB-AC* increased from 63.5 to 83.1 mg·g^{-1} and from 76.8 to 87.7 mg·g^{-1} as the temperature increased from 15 to 45°C for BPA and TCP, respectively. The data indicate that the adsorption process of BPA and TCP onto *A-OAB-AC* was favored at higher temperature, in agreement with an endothermic adsorption process. This was due to a higher affinity of adsorbent for the both adsorbates or the increasing in the number of active sites on the *A-OAB-AC* surface [27]. The endothermic nature of adsorption was similarly reported for removal of 2,4-dichlorophenoxyacetic and hydroxy-Al from aqueous solution using activated carbon [48], and montmorillonite [49].

3.8. Thermodynamics of adsorption

The thermodynamic parameters reflect the feasibility and the spontaneous nature of a sorption process. Four different temperatures, 288, 298, 308 and 318 K were studied for the determination of thermodynamic parameters of adsorption, such as Gibb's free energy (ΔG°), enthalpy change (ΔH°), and entropy change (ΔS°) are calculated at different temperatures using the following equations:

$$\Delta G^\circ = -RT\,Ln\,1000 * K \tag{12}$$

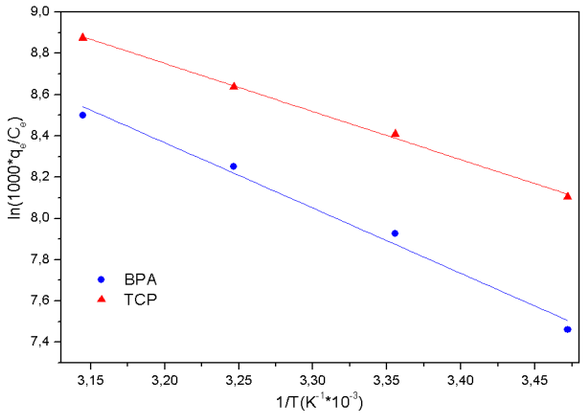

Fig. 8. Vant Hoff's plot for the adsorption of BPA and TCP by *A-OAB-AC*.

Table 4
Thermodynamic parameters for adsorption of BPA and TCP onto A-OAB-AC

Toxic pollutants	T(K)	ΔG° (kJ·mol^{-1})	ΔH° (kJ·mol^{-1})	ΔS° (J·mol^{-1} K^{-1})
BPA	288	–17.97	26.3	153.80
	298	–19.51		
	308	–21.05		
	318	–22.58		
TCP	288	–19.43	19.4	134.80
	298	–20.78		
	308	–22.13		
	318	–23.48		

$$Log\left(\frac{1000 \times q_e}{C_e}\right) = \frac{\Delta S^0}{2.303R} - \frac{\Delta H^0}{2.303RT} \tag{13}$$

Where q_e is the amount of BPA and TCP adsorbed per unit mass of *A-OAB-AC* (mg·g^{-1}), C_e is the equilibrium concentration (mg·L^{-1}), R is the universal gas constant (8.314 J·K^{-1}·mol^{-1}), t is the temperature in Kelvin (K) and K is the equilibrium constant for BPA/TCP between the solution and the adsorbent surface. From the plot of Log (1000 × q_e/C_e) vs. 1/T (Fig. 8), the intercept and slope were used to determine the values of ΔH° and ΔS°, respectively. The thermodynamic adsorption parameters determined are summarized in Table 4. All ΔG° values are negative and increase with increasing temperature, indicating that the BPA or TCP adsorption process on *A-OAB-AC* was spontaneous. Additionally, the magnitude of ΔG° may also give an idea about the nature of adsorption process whether it is chemisorption (i.e. –400 to –80 kJ mol^{-1}) or physisorption (i.e. –20 to 0.0 kJ mol^{-1}) [24]. The obtained values of ΔG° for the adsorption of BPA and TCP using *A-OAB-AC* were within the ranges of -17.9 to -22.6 kJ mol^{-1} and –19.4 to –23.5 kJ mol^{-1}, respectively. The obtained results do not fall into a range of pure chemical adsorption process, indicating a

Table 5
Comparison of the monolayer adsorption capacity of BPA and TCP by various adsorbents

Adsorbate	Adsorbent	q_{max} (mg·g^{-1})	Ref
BPA	A-OAB-AC	368.2	This study
	Organo-acid-activated bentonite	127.7	[4]
	Activated carbon prepared from olive-mill waste	399.5	[18]
	Commercial activated carbon	164.4	[18]
	Cationic-modified zeolite	37.8	[46]
	Hybrid multi-willed carbon nanotubes-alginate-polysolfone	24.5	[47]
	Organo-montmorillonite	114.9	[48]
TCP	A-OAB-AC	385.1	This study
	Organo-acid activated bentonite	244.6	[4]
	Organophilic-bentonite	72.2	[25]
	β-cyclodextrinmesoporous attapulgite composites	65.2	[45]
	Modifiednatural bentonite	160.4	[49]
	MgAl-SDBS organo-layered double hydroxides	240.5	[50]

combination of physisorption and chemisorption where the former is the dominating mechanism. The positive ΔH° values (26.3 and 19.4 kJ·mol^{-1}) of both BPA and TCP adsorption on *A-OAB-AC* confirmed the involvement of an endothermic process. The values of enthalpy changes ΔH° were lower than 84 kJ·mol^{-1}, which indicate a physisorption adsorption process. Also the positive values of entropy changes (ΔS°) (153.8 and 134.8 J·K^{-1}·mol^{-1} for BPA and TCP, respectively) show, randomness nature of process at the solid/solution interface and the affinity of *A-OAB-AC* for BPA and TCP adsorption [24,27,50].

3.9. Comparison of adsorption of BPA and TCP on various adsorbents

Table 5 presents the comparison of the maximum adsorption capacity of the BPA and TCP monolayer on different adsorbents. Based on the recorded data, it can be concluded that the efficiency of BPA and TCP adsorption on the adsorbent tested in this study(*A-OAB-AC*) was greater than that obtained for the other adsorbents. *A-OAB-AC* is more reliable alternative adsorbent in terms of high capacity efficiency and fast adsorption rate.

3.10. Desorption and regeneration of A-OAB -AC

Regeneration studies were carried out in order to know the reusability of the adsorbent because one of the extremely essential ways to economically assess a good adsorbent is its reusability qualities [29,52]. To investigate the reusability of *A-OAB-AC* as adsorbent for BPA and TCP removal, six cycles of desorption/adsorption were undertaken with ethanol desorbing agent. Six regeneration adsorption capacities of *A-OAB-AC* are shown in Fig. 9, for two toxic pollutants. It was observed that at the first adsorption step, the adsorption capacities for the BPA and TCP reached the values of 76.0 and 82.9 mg·g^{-1}, respectively. After six cycles, the adsorption capacity of *A-OAB-AC* adsorbent decreased from 76.0 to 62.0 and from 82.9 to 73.3 mg·g^{-1} for BPA and TCP, respectively. As seen from the figure, the total adsorption capacities of both BPA and TCP slightly decreased after six-time regeneration; not more than 18 and 11% when compared with the virgin adsorption capacity for BPA and TCP, respectively. This could be ascribed to the fact that the regeneration process might result in the decrease of binding sites [5,24,27]. The obtained data from the adsorption–desorption tests illustrate efficient and stabilized performance of *A-OAB-AC* in repeated cycles. This also proves that *A-OAB-AC* is a promising material that could be used successfully for pollution remediation.

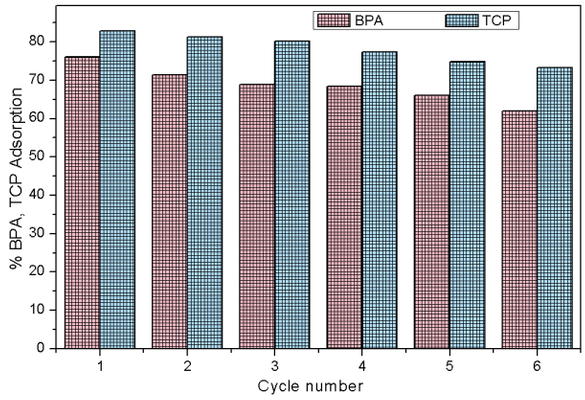

Fig. 9. Histogram of regeneration test for the adsorption of BPA and TCP onto *A-OAB-AC* adsorbent.

4. Conclusion

The newly prepared eco-friendly composite hydrogel (*A-OAB-AC*) showed high adsorption capacities for the removal of BPA (368.2 mg·g^{-1}) and TCP (385.0 mg·g^{-1}) from aqueous solution. The kinetics of the adsorption followed pseudo second-order equation. The mechanism involved both chemical and physical processes. Freundlich model showed satisfactory fit to the equilibrium adsorption data of *A-OAB-AC* composite. After adsorption, the interaction between the adsorbates and the composite was confirmed by FTIR spectroscopy. The thermodynamic study showed that the adsorption process was spontaneous and endothermic. The composite displayed an excellent regeneration capacity; it may be used as a promising adsorbent and shall be recommended for testing in larger scale industrial facilities.

References

[1] N.R. Hendricks, T.T. Waryo, O. Arotiba, N. Jahed, P.G.L. Baker, E.I. Iwuoha, Microsomal cytochrome P450-3A4 (CYP3A4) nanobiosensor for the determination of 2,4-dichlorophenol—An endocrine disruptor compound, Electrochim.Acta., 54 (2009) 1925–1931.

[2] S. Rovani, M.T. Censi, Sidnei L.P. Jr É. C. Lima, R. Cataluna, A.N. Fernandes, Development of a new adsorbent from agro-industrial waste and its potential use in endocrine disruptor compound removal, J. Hazard. Mater., 271 (2014) 311–320.

[3] J.Y. Park, J.H. Choi, A.M. Abd El-Aty, B.M. Kim, J.H. Park, W.J. Choi, J.H. Shim, Development and validation of an analytical method for determination of endocrine disruptor, 2,4-D, in paddy field water, Biomed. Chromatogr., 25 (2011) 1018–1024.

[4] N. Djebri, M. Boutahala, N. Chelali, N. Boukhalfa, L. Zerroual, Adsorption of bisphenol A and 2,4,5-trichlorophenol onto organo-acid-activated bentonite from aqueous solutions in single and binary systems, Desal. Water Treat., 66 (2017) 383–393.

[5] N. Djebri, M. Boutahala, N. Chelali, N. Boukhalfa, L. Zeroual, Enhanced removal of cationic dye by calcium alginate/organobentonite beads: Modeling, kinetics, equilibriums, thermodynamic and reusability studies, Int. J. Biol. Macromol., 92 (2016) 1277–1287.

[6] A. Huan, H. Chen, L. Chen, Y. Dai, J. Zhao, Effects of Cd(II) and Cu(II) on microbial characteristics in 2-chlorophenol-degradation anaerobic bioreactors, J. Environ. Sci., 20 (2008) 745–752.

[7] X. Wang, J. Yang, Y. Wang, Y. Li, F. Wang, L. Zhang, Studies on electrochemical oxidation of estrogenic disrupting compound bisphenol AF and its interaction with human serum albumin, J. Hazard. Mater., 276 (2014) 105–111.

[8] R.S. Juang, W.C. Huang, Y.H. Hsu, Treatment of phenol in synthetic saline wastewater by solvent extraction and two-phase membrane biodegradation, J. Hazard. Mater., 164 (2009) 46–52.

[9] A. Hashem, Hamdy A. Hammad, A. Al-Anwar, Modified Camelorum tree particles as a new adsorbent for adsorption of Hg(II) from aqueous solutions: kinetics, thermodynamics and non-linear isotherms, Desal. Water Treat., 57 (2016) 23827–23843.

[10] D. Tabassi, A. Mnif, B. Hamrouni, Influence of operating conditions on the retention of phenol in water by reverse osmosis SG membrane characterized using Speigler–Kedem model, Desal. Water Treat., 52 (2014) 1792–1803.

[11] S. Das, S. Garrison, S. Mukherjee, Bi-functional mechanism in degradation of toxic water pollutants by catalytic amorphous metals, Adv. Eng. Mater., 18 (2016) 214–218.

[12] A.H. Jawad, R.A. Rashid, M.A. MohdIshak, D.L. Wilson, Adsorption of methylene blue onto activated carbon developed from biomass waste by H_2SO_4 activation: kinetic, equilibrium and thermodynamic studies, Desal. Water Treat., 57 (2016) 25194–25206.

[13] A. Emami, A.R. Kelishami, Zinc and nickel adsorption onto a low-cost mineral adsorbent: kinetic, isotherm, and thermodynamic studies, Desal. Water Treat., 57 (2016) 21881–21892.

[14] M. J. Ahmed, S.K. Theydan, Equilibrium isotherms, kinetics and thermodynamics studies of phenolic compounds adsorption on palm-tree fruit stones, Ecotoxicol. Environ. Saf., 84 (2012) 39–45.

[15] F.S. Hashem, M.S. Amin, Adsorption of methylene blue by activated carbon derived from various fruit peels, Desal. Water Treat., 57 (2016) 22573–33584.

[16] I.A.W. Tan, A.L. Ahmad, B.H. Hameed, Adsorption of basic dye on high-surface-area activated carbon prepared from coconut husk: Equilibrium, kinetic and thermodynamic studies, J. Hazard. Mater., 154 (2008) 337–346.

[17] C. Djilani, R. Zaghdoudi, A. Modarressi, M. Rogalski, F. Djazi, A. Lallam, Elimination of organic micropollutants by adsorption on activated carbon prepared from agricultural waste, Chem. Eng. J., 189– 190 (2012) 203– 212.

[18] M.I. Bautista-Toledo, J. Rivera-Utrilla, R. Ocampo-Perez, F. Carrasco-Marın, M. Sanchez-Polo, Cooperative adsorption of bisphenol-A and chromium(III) ions from water on activated carbons prepared from olive-mill waste, Carbon, 73 (2014) 338–350.

[19] R. Baccar, M. Sarrà, J. Bouzid, M. Feki, P. Blánquez, Removal of pharmaceutical compounds by activated carbon prepared from agricultural by-product, Chem. Eng. J., 211–212 (2012) 310–317.

[20] S. Saeidnia, G. AsadollahFardi, A.K. Darban, Simulation of adsorption of antimony on zero valent iron nanoparticles coated on the industrial minerals (kaolinite, bentonite and perlite) in mineral effluent, Desal. Water Treat., 57 (2016) 22321–22328.

[21] S. Şimşek, Adsorption properties of lignin containing bentonite–polyacrylamide composite for ions, Desal. Water Treat., 57 (2016) 23790–23799.

[22] A.F. Hassan, A.M. Abdel-Mohsen, M.M.G. Fouda, Comparative study of calcium alginate, activated carbon, and their composite beads on methylene blue adsorption, Carbohydr. Polym.,102 (2014) 192– 198.

[23] M.J.C. Calagui, D.B. Senoro, C.C. Kan, J.W.L. Salvacion, C.M. Futalan, M.W. Wan, Adsorption of indium(III) ions from aqueous solution using chitosan-coated bentonite beads, J. Hazard. Mater., 277 (2014) 120–126.

[24] A.A. Oladipo, M. Gazi, Enhanced removal of crystal violet by low cost alginate/acid activated bentonite composite beads: Optimization and modelling using non-linear regression technique, J. Water. Process. Eng., 2 (2014) 43–52.

[25] Y. Sun, Q. Yue, B. Gao, L. Huang, X. Xu, Q. Li, Comparative study on characterization and adsorption properties of activated carbons with H_3PO_4 and $H_4P_2O_7$ activation employing Cyperusalternifolius as precursor, Chem. Eng. J., 181–182 (2012) 790– 797.

[26] M. Benadjemia, L. Millière, L. Reinert, N. Benderdouche, L. Duclaux, Preparation, characterization and Methylene Blue adsorption of phosphoric acidactivated carbons from globe artichoke leaves, Fuel Proces. Technol., 92 (2011) 1203–1212.

[27] L. Xiaona, C. Shuo, F. Xinfei, Q. Xie, T. Feng, Z. Yaobin, G. Jinsuo, Adsorption of ciprofloxacin, bisphenol and 2-chlorophenol on electrospun carbon nanofibers: In comparison with powder activated carbon, J. Colloid Interface Sci., 447 (2015) 120–127.

[28] S.K. Nadavala, K. Swayampakula, V.M. Boddu, K. Abburi, Biosorption of phenol and *o*-chlorophenolfrom aqueous solutions on to chitosan–calcium alginate blended beads, J. Hazard. Mater., 162 (2009) 482–489.

[29] S.N. AeisyahAbas, M.H. Shah Ismail, S.I. Siajam, M.L. Kamal, Development of novel adsorbent-mangrove-alginate composite bead (MACB) for removal of Pb(II) from aqueous solution, J. Taiwan. Inst. Chem. Eng., 000 (2015) 1–8.

[30] Y.H. Kim, B. Lee, K.H. Choo, S.J. Choi, Selective adsorption of bisphenol A by organicinorganic hybrid mesoporoussilicas, Micropor. Mesopor. Mater., 138 (2011) 184–190.

[31] H.Z. Boudiaf, M. Boutahala Equilibrium and kinetics studies of 2,4,5-trichlorophenol adsorption onto organophilic-bentonite, Desal. Water Treat., 24 (2010) 47–54.

[32] S. Sahnoun, M. Boutahala, H.Z. Boudiaf, L. Zerroual, Trichlorophenol removal from aqueous solutions by modified halloysite: kinetic and equilibrium studies, Desal. Water Treat., 57 (2015) 15941–15951.

[33] H.Z. Boudiaf, M. Boutahala, Kinetic analysis of 2,4,5-trichlorophenol adsorption onto acid-activated montmorillonite from aqueous solution, Int. J. Miner. Process., 100 (2011) 72–78.

[34] N. Boukhalfa, M. Boutahala, N. Djebri, Synthesis and characterization of ZnAl-layered double hydroxide and organo-K10 montmorillonite for the removal of diclofenac from aqueous solution, Adsorpt. Sci. Technol., 0(0) (2016) 1–17.

[35] H.L. Pam, L.B. Roderick, D.H. Malcolm, A pseudo first order rate model for the adsorption of an organic adsorbate in aqueous solution, J. Chem. Technol. Biotechnol., 74 (1999) 55–59.

[36] S. Chowdhury, P. Saha, Adsorption kinetic modeling of safranin onto rice husk biomatrix using pseudo-first- and pseudo-second-order kinetic models: comparison of linear and non-linear methods, Clean – Soil, Air, Water, 39(3) (2011) 274–282.
[37] J. Febrianto, A.N. Kosasih, J. Sunarso, Y.H. Ju, N. Indraswati, S. Ismadji, Equilibrium and kinetic studies in adsorption of heavy metals using biosorbent: A summary of recent studies, J. Hazard. Mater., 162 (2009) 616–645.
[38] M. Ghaedi, R. Hassani, K. Dashtian, G. Shafie, M.K. Purkait, H. Dehghan, Adsorption of methyl red onto palladium nanoparticles loaded on activated carbon: experimental design optimization, Desal. Water Treat., 57 (2016) 22646–22654.
[39] Z. Cheng, R. Yang, X. Zhu, Adsorption behaviors of the methylene blue dye onto modified sepiolite from its aqueous solutions, Desal. Water Treat., 57 (2016) 25207–25215.
[40] M. Perez-Ameneiro, X. Vecino, L. Barbosa-Pereira, J.M. Cruz, A.B. Moldes, Removal of pigments from aqueous solution by a calciumalginate–grape marc biopolymer: A kinetic study, Carbohydr. Polym., 101 (2014) 954– 960.
[41] M. Perez-Ameneiro, X. Vecino, J.M. Cruz, A.B. Moldes, Wastewater treatment enhancement by applying a lipopeptide biosurfactant to a Lignocellulosic biocomposite, Carbohydr. Polym., 131 (2015) 186–196.
[42] M. Perez-Ameneiro, G. Bustos, X. Vecino, L. Barbosa-Pereira, J.M. Cruz, A.B. Moldes, Heterogeneous lignocellulosic composites as bio-based adsorbents for wastewater dye removal: a kinetic comparison, Water Air Soil Pollut., 226 (2015) 133.
[43] M. Perez-Ameneiro, X. Vecino, J.M. Cruz, A.B. Moldes, Physicochemical study of a bio-based adsorbent made from grape marc, Ecol. Eng., 84 (2015) 190–193.
[44] I. Langmuir, The constitution and fundamental properties of solids and liquids, J. Am. Chem. Soc., 38 (1916) 2221–2295.
[45] T.W. Weber, R.K. Chkraborti, Pore, solid diffusion models for fixed bed adsorbers, Am. Inst. Chem. Eng. J., 20 (1974) 228–238.
[46] Q. Peng, M. Liu, J. Zheng, C. Zhou, Adsorption of dyes in aqueous solutions by chitosan–halloysite nanotubes composite hydrogel beads, Micropor. Mesopor. Mater., 201 (2015) 190–201.
[47] X. Vecino, R.D. Rey, S. Villagrasa, J.M. Cruz1, A.B. Moldes, Kinetic and morphology study of alginate-vineyard pruning waste biocomposite vs. non modified vineyard pruning waste for dye removal, J. Environ. Sci., 38 (2015) 158–167.
[48] V.O. Njoku, B.H. Hameed, Preparation and characterization of activated carbon from corncob by chemical activation with H_3PO_4 for 2,4-dichlorophenoxyacetic acid adsorption, Chem. Eng. J., 173 (2011) 391–399.
[49] G. Wang, X. Sud, Y. Hua, S. Ma, J. Wang, X. Xue, Q. Tao, S. Komarneni, Kinetics and thermodynamic analysis of the adsorption of hydroxy-Al cations by montmorillonite, Appl. Clay. Sci., 129 (2016) 79–87.
[50] X. Zheng, J. Dai, J. Pan, Synthesis of β-cyclodextrin/mesoporous attapulgite composites and their novel application in adsorption of 2,4,6-trichlorophenol and 2,4,5-trichlorophenol, Desal. Water Treat., 57 (2016) 14241–14250.
[51] H. Wang, H. Zhang, J.Q. Jiang, X. Ma, Adsorption of Bisphenol A onto cationic-modified Zeolite, Desal. Water Treat., 57 (2016) 26299–26306.
[52] M.R. Hartono, R.S. Marks, X. Chen, A. Kushmaro, Hybrid multi-walled carbon nanotubes-Alginate-Polysulfone beads for adsorption of Bisphenol-A from aqueous solution, Desal. Water Treat., 54 (2015) 1167–1183.
[53] Y. Park, Z. Sun, G.A. Ayoko, R.L. Frost, Bisphenol A sorption by Organo-Montmorillonite: Implications for the removal of organic contaminants from water, Chemosphere, 107 (2014) 249–25.
[54] H.Z. Boudiaf, M. Boutahala, S. Sahnoun, C. Tiar, F. Gomri, Adsorption characteristics, isotherm, kinetics, and diffusion of modified natural bentonite for removing the 2,4,5-Trichlorophenol, Appl. Clay Sci., 90 (2014) 81–87.
[55] H.Z. Boudiaf, M. Boutahala, C. Tiar, L. Arab, F. Garin, Treatment of 2,4,5-Trichlorophenol by MgAl–SDBS Organo-Layered double hydroxides: Kinetic and equilibrium studies, Chem. Eng. J., 173 (2011) 36–41.